International Journal of Nanomedicine

Dovepress
Taylor & Francis Group

Open Access Full Text Article

ORIGINAL RESEARCH

A Targeted Nanotoxin Inhibits Colorectal Cancer Growth Through Local Tumor Pyroptosis and Eosinophil Infiltration and Degranulation

Luis Miguel Carrasco-Díaz[1–3], Alberto Gallardo[4], Eric Voltà-Durán[3,5,6], Anna C Virgili[1,7], David Páez[7,8], Antonio Villaverde[3,5,6], Esther Vazquez[3,5,6], Patricia Álamo[1–3], Ugutz Unzueta[1–3,6], Isolda Casanova[1–3], Ramon Mangues[1–3,*], Lorena Alba-Castellon[1–3,*]

[1]Onco-Hematological Diseases Department, Institut de Recerca SANT Pau (IR Sant Pau), Barcelona, Spain; [2]Myeloid Neoplasms Program, Josep Carreras Leukaemia Research Institute (IJC Sant Pau), Barcelona, Spain; [3]CIBER de Bioingeniería, Biomateriales y Nanomedicina (CIBER-BBN), Madrid, Spain; [4]Department of Pathology, Hospital de la Santa Creu I Sant Pau, Barcelona, Spain; [5]Institut de Biotecnologia i de Biomedicina, Universitat Autònoma de Barcelona, Bellaterra, Spain; [6]Departament de Genètica i de Microbiologia, Universitat Autònoma de Barcelona, Bellaterra, Spain; [7]Department of Medical Oncology, Hospital de la Santa Creu I Sant Pau, Barcelona, Spain; [8]CIBER de Enfermedades Raras (CIBERER), Madrid, Spain

*These authors contributed equally to this work

Correspondence: Ramon Mangues, Lorena Alba-Castellon, Institut de Recerca Sant Pau (IR SANT PAU), Sant Quintí 77-79, Barcelona, 08041, Spain, Email rmangues@santpau.cat; lalba@santpau.cat

Background: Colorectal cancer (CRC) has traditionally been treated with genotoxic chemotherapy to activate pro-apoptotic proteins to induce anticancer effects. However, cancer cells develop resistance to apoptosis, which leads to recurrence and poor prognosis. Moreover, this kind of therapy has been shown to be highly toxic to healthy tissues and, therefore, to patients. To overcome this issue, we developed a self-assembly tumor-targeted nanoparticle, T22-DITOX-H6, that incorporates the T22 peptide (a CXCR4 ligand) to selectively target cells overexpressing CXCR4, fused to the catalytic domain of diphtheria toxin, that exhibits a potent cytotoxic effect on these CXCR4+ cancer cells that exhibits potent cytotoxic effects on CXCR4-overexpressing cancer cells through the activation of pyroptosis, an immunogenic type of cell death.

Methods: Colorectal CXCR4-expressing tumor cells (CT26-CXCR4+) were implanted subcutaneously into immunocompetent mice to study the effects of T22-DITOX-H6 treatment on tumor growth, cell death and innate immune cell recruitment to the tumor.

Results: Here, we demonstrated that the T22-DITOX-H6 nanoparticle selectively activated pyroptosis, an immunogenic cell death that differs from apoptosis, leading to cell death in CXCR4-expressing cells, without affecting the viability of CXCR4-lacking cells. In addition, the nanoparticle administered to tumor-bearing mice induced a local antitumor effect due to the selective activation of pyroptosis in CXCR4+ targeted cancer cells. Biochemical analysis of plasma and histological analysis of non-tumor tissues revealed no differences between the groups. Remarkably, pyroptosis activation stimulates eosinophil infiltration into the tumor microenvironment, an effect recently reported to have an anti-tumorigenic function.

Conclusion: These results highlight the dual role of CXCR4-targeted cytotoxic nanoparticle in eliminating cancer cells and boosting the self-immune response without compromising healthy organs.

Keywords: solid tumor, targeted therapy, innate immune response, protein-only nanoparticle

Introduction

Colorectal cancer (CRC) has mainly been treated for decades with genotoxic chemotherapy. It consists of a combination of lipophilic untargeted small drugs (5-Fluorouracil, Irinotecan, Oxaliplatin)[1] aiming to induce anticancer effects through the activation of pro-apoptotic proteins. In cancer tissues, cancer stem cells (CSCs) maintain tumor growth and metastatic dissemination, as well as capable of developing resistance to chemotherapy, mostly by upregulation of Bcl2 anti-apoptotic proteins,[2] which leads to recurrence and poor prognosis.[3,4]

Received: 3 October 2024
Accepted: 14 January 2025
Published: 26 February 2025

Graphical Abstract

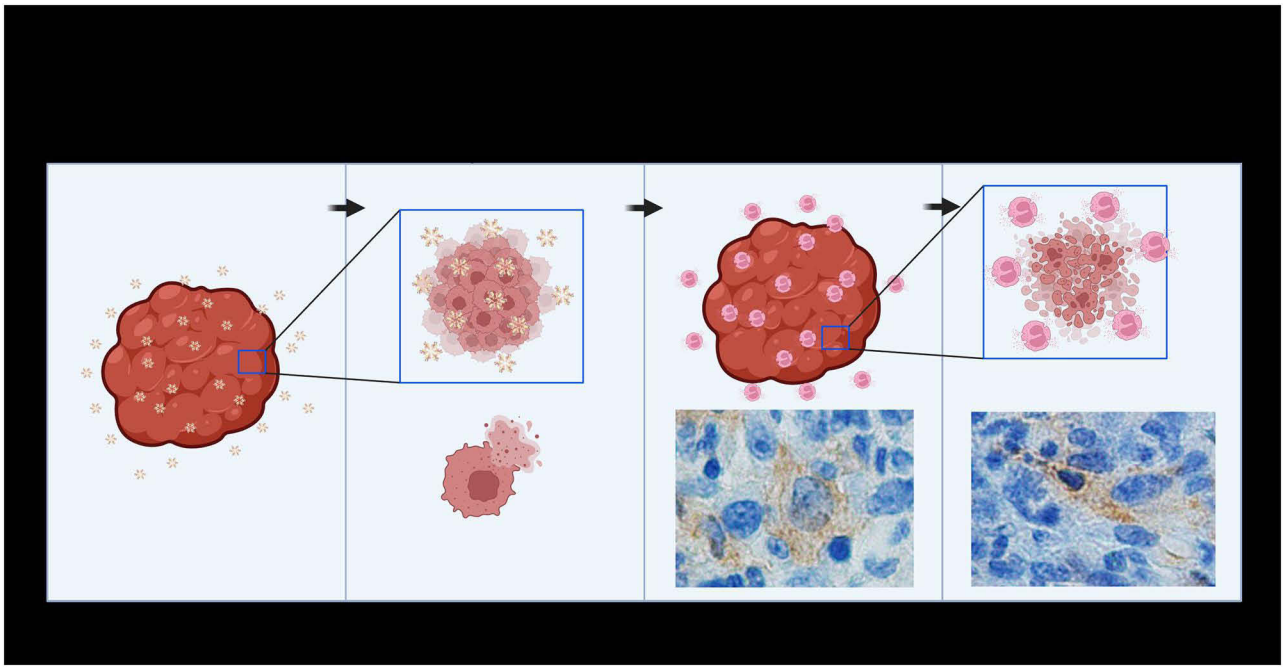

Moreover, these hydrophobic drugs cross cell membranes and are biodistributed throughout the body, reaching cancer and normal cells. Thus, their high toxicity limits their dosage.[5] Recently, Pembrolizumab, an immune checkpoint inhibitor (ICI), has been approved for first line treatment in patients with microsatellite instability (MSI) colorectal cancer.[6] However, most of diagnosed colorectal cancer patients present microsatellite stability (MSS), and there are no markers in MSS CRC that can predict the response to ICI.[7] Therefore, new anticancer approaches are urgently needed to achieve selective targeting of CSCs to increase antitumor activity with high safety for most of the CRC patients.

Our group has previously generated the T22-DITOX-H6 nanotoxin, a fusion protein delivery system designed to selectively release a bacterial toxin into the cytosol of cancer cells that overexpress the CXCR4 receptor (CXCR4+) on their membrane. The nanotoxin is composed of self-assembled monomers with three functional domains: the T22 ligand, which specifically binds to CXCR4 and triggers receptor-mediated endocytosis; the catalytic and translocation domains of the *Corynebacterium diphtheriae* exotoxin, flanked by furin cleavage sites; and a polyhistidine tail. Upon internalization into CXCR4+ cells via endocytosis, endosomal furins release the bacterial toxin, which translocates into the cytoplasm through its translocation domains. Once in the cytosol, the catalytic domain inhibits protein synthesis by targeting eukaryotic elongation factor 2 (EF-2); inducing cell death. Thus, this oligomeric nanotoxin achieves highly selective internalization into CXCR4+ cells and efficient cytosolic release of the exotoxin by avoiding its lysosomal degradation, ensuring targeted cancer cell killing[8–10] (Figure 1a).

Moreover, we recently reported a potent anticancer effect due to induction of pyroptosis in CXCR4+ cells in CRC mouse models. CXCR4 expression has been related to higher metastatic dissemination and poor prognosis in different cancer types, including CRC. Additionally, it is expressed by CSCs;[11,12] thus, a therapy targeting CXCR4+ cells have the potential to eliminate CSCs along with cancer cells.[8,9]

Pyroptosis is an inflammatory cell death mechanism, alternative to apoptosis, and barely explored in cancer therapy. We found that repeated injection of the nanotoxin T22-DITOX-H6 induced pyroptosis, leading to anticancer effects without associated systemic toxicity in immunosuppressed CXCR4+ CRC models.

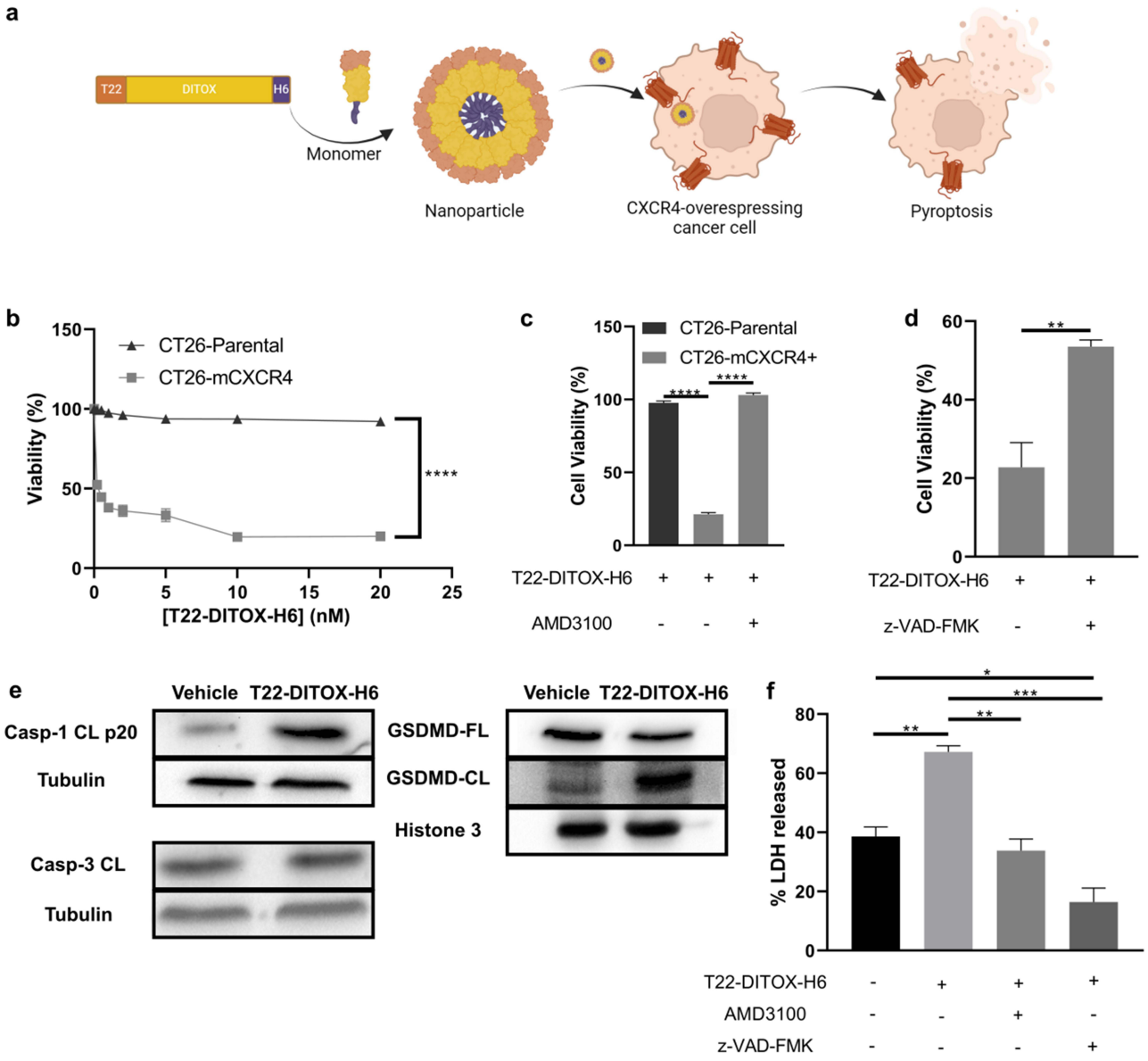

Figure 1 T22-DITOX-H6 CXCR4-dependent cytotoxic effects in mouse CT26 cell line. (**a**) Schematic representation of nanotoxin T22-DITOX-H6 which is formed by monomers that contain the ligand domain T22, which recognizes the CXCR4 receptor; the cytotoxic domain, DITOX; and a histidine tail, H6, which allows protein purification. (**b**) Cell viability assay performed 48 hours after exposing CT26-Parental and CT26-mCXCR4+ cell lines to increasing concentrations of T22-DITOX-H6. (**c** and **d**) Cell viability assay to demonstrate CXCR4 (**c**) and caspase (**d**) dependence on the cytotoxic activity of T22-DITOX-H6 (10 nM) for 48h. When indicated, cells were treated with AMD3100 (100 nM), a CXCR4 antagonist, or z-VAD-FMK (100 μM), a pan-caspase inhibitor, prior to T22-DITOX-H6 for 1h. (**e**) Representative images of cleaved caspase-1 p20, cleaved caspase-3, GSDMD, and cleaved N-terminal GSDMD immunoblotting of protein extracts from CT26-mCXCR4+ cells treated with either vehicle or T22-DITOX-H6 (10 nM) for 24h. Tubulin and Histone 3 were used as a loading control. (**f**) Quantification of LDH released into the supernatant of cultured CT26-mCXCR4+ cells treated with T22-DITOX-H6 (10 nM) for 48h. Cells were treated with either AMD3100 (100 nM) or z-VAD-FMK (100 μM) for 1h when indicated. **** $p<0.0001$; *** $p<0.001$; ** $p<0.01$; * $p<0.05$. Each column represents the mean value of three biological replicates. Error bars indicate ±SEM.

This exciting discovery triggered the generation of syngeneic CXCR4+ CRC models to test if inflammation induced by pyroptosis engages the immune system against the tumor in immunocompetent mice. Thus, contrary to non-immunogenic apoptosis, the targeted release of the exotoxin of *C. diphtheriae* in target cancer cells activates the inflammasome, through NLRP3-dependent pyroptosis which is highly inflammatory and immunogenic.[13]

Here, we evaluated whether immunogenicity induced by diphtheria exotoxin was able to engage eosinophils in killing epithelial cancer cells in tumor tissue, based on three kinds of previous evidence. First, epithelial cells infected by bacteria release exotoxins that attract eosinophils to the infected tissue, triggering degranulation; that is, the secretion of proteins that kill infected epithelial cells to control the disease.[14–16] Second, inflamed intestinal epithelial cells infected

https://doi.org/10.2147/IJN.S499192

by intruding bacteria are killed by resident eosinophils to maintain the barrier function. Finally, eosinophil infiltration in CRC tumors improves patient prognosis.[17–22]

In this study, we found that CXCR4-targeted T22-DITOX-H6 multivalent nanotoxin was able to induce anticancer effect through selective pyroptosis in local tumor, mediated by caspase-1 activation and GSDMD cleavage. This was followed by eosinophil infiltration and degranulation in the tumor tissue in an immunocompetent CXCR4+ CRC model. Importantly, the local tumor distribution of previous targeted nanotoxin therapy can induce selective cell death in CXCR4+ cancer cells within the tumor, with negligible uptake and toxicity in normal cells, as we had previously reported in five different cancer models.[9,23–26] Consistently, we found a significant local eosinophil degranulation in tumor tissue associated with a high antitumor effect, in the absence of systemic toxicity, opening an anticancer strategy able to induce local immunogenic therapy only in cancer tissue, an alternative to current chemotherapy in CRC.

Furthermore, our CXCR4-targeted therapy that activates pyroptosis represents an innovative solution of great interest for patients who do not respond to immunotherapy treatments. Additionally, merging this anticancer agent that induce pyroptosis with immunotherapy drugs to create synergistic antitumor effects is evolving into a promising strategy.

Materials and Methods

Nanotoxin

T22-DITOX-H6 nanoparticle production, purification and characterization have been previously described.[10] Briefly, the T22-DITOX-H6 nanoparticle is a recombinant protein produced in the *Escherichia coli* Origami B strain and purified by Immobilized Metal Affinity Chromatography (IMAC) using a HiTrap Chelating HP 1 mL column (GE Healthcare, New Jersey, USA). The structure of the nanotoxin consists of monomers that self-assemble into nanoparticles of 38 and 90 nm. The monomers forming the nanoparticles are composed of the T22 ligand, a CXCR4 antagonist peptide that binds and is internalized by this receptor. The T22 peptide is genetically fused with DITOX, which contains the translocation and catalytic domains of the diphtheria toxin from *Corynebacterium diphtheriae*. Finally, at the C-terminal of the monomer, a 6-histidine tag is fused, which participates in the self-assembly of the nanoparticle by interacting with other histidine tags. Additionally, the H6 tag is necessary for protein purification.

Cell Lines and Cell Culture

CT26 cell line was purchased from ATCC (CRL-2638, ATCC; Manassas, USA). CT26 cell line was cultured in medium Roswell Park Memorial Institute (RPMI) 1640 (Gibco, Life Technologies, Waltham, USA) supplemented with 10% Fetal Bovine Serum (FBS), 100 U/mL penicillin/streptomycin, and 2mM glutamine (Gibco, Life Technologies, Waltham, USA) and incubated at 37°C and 5% CO2 in a humidified atmosphere.

CT26-mCXCR4+ cell line was obtained as follows: CT26 cells (Parental CT26, CT26-Par) were transduced with pLV-EF1A-Puro-mCXCR4 (VectorBuilder Chicago, USA) as previously described.[21] Briefly, viral particles were produced in 293t cells by co-transfection of pLV-EF1A-Puro-mCXCR4, pMD.G-VSV G-poly-A vector and p8.91-Gag-Pol vectors and added to 2.5×10^6 CT26-Parental cells for 48 h. Transduced cells, CT26-mCXCR4+ were selected in medium containing puromycin (1 µg/mL) for 2 weeks. Then, selected CT26-mCXCR4+ cells were sorted by mCXCR4 membrane expression (FACSAria cell sorter (BD Bioscience, Franklin Lakes, USA)) using PE rat anti-mouse CD184 (mCXCR4) antibody (#146505, Biolegend, San Diego, USA).

Detection of CXCR4 Membrane Expression

CT26 murine cell line was cultured and trypsinized at 80% of confluence. Cells were washed with PBS-0.5% Bovine Serum Albumin (BSA). Then, 10^6 cells in 100 µL were incubated 20 min at 4 °C with 2.5 µL of PE rat anti-mouse CD184 (mCXCR4) antibody (#146505, Biolegend, San Diego, USA) or PE rat IgG2b isotype control antibody (#400607, Biolegend, San Diego, USA). Afterwards, cells were washed with PBS-0.5% BSA, resuspended in PBS-0.5% BSA and analyzed by FACS Calibur cytometer (BD Bioscience, Franklin Lakes, USA).

Cell Viability Assays

Cell Proliferation Kit II (XTT) (#11465015001, Roche Diagnostics, Basel, Switzerland) was used according to the manufacturer's instructions. Cells were seeded in 96-well plates (5000 cells/well) and treated with either T22-DITOX-H6 (0.2 nM to 20 nM) or vehicle (166 mm NaCO3H pH 8.0), when referring to 0 nM treated cells, for 48 h. When indicated, cells were pre-treated 1 h before nanotoxin addition with 100 nM AMD3100 (Sigma-Aldrich, Burlington, USA) or 100 μM z-VAD-FMK (Selleckchem, Houston, USA). Forty-eight hours after T22-DITOX-H6 treatment, XTT reagent was added and measured at 492 nm (FLUOstar OPTIMA spectrophotometer (BMG Labtech, Ortenberg, Germany)) after 4 h of incubation at 37° C.

LDH Release Assay

Cells were seeded in 96-well plates (5000 cells/well) and exposed to 10 nM T22-DITOX-H6 for 48 h. AMD3100 and z-VAD-FMK pre-treatment were added at 100 nM and 100 μM, respectively, and incubated at 37° C for 1 h before T22-DITOX-H6 addition. LDH release into the supernatant was measured using the Cytotox 96 Non-Radioactive Cytotoxicity Assay (G1782, Promega, Madison, USA) according to the manufacturer's instruction.

Western Blot

In order to obtain cell extracts, 5.0×10^5 CT26-mCXCR4+ cells were seeded in petri dish (Sigma-Aldrich, Burlington, USA) and treated with either vehicle or 10 nM of T22-DITOX-H6 for 24 h. After incubation time, cells were washed twice with cold Phosphate Buffered Saline (PBS) and resuspended in Sodium Dodecyl Sulfate (SDS) lysis buffer (0.05 M Tris-HCl pH 6.8, 2% SDS, 10% glycerol). Cells were lysed passing the cell suspension through a 27-G syringe ten times, and then the suspension was centrifuged for 10 min at 21,000 *g* at 4°C. Whole-cell protein extracts were quantified (BCA Gold Protein Quantification kit (A53225, Thermo Fisher Scientific, Waltham, USA)), and 40 μg of proteins were used for SDS-Polyacrylamide Gel Electrophoresis (PAGE) electrophoresis. Proteins were transferred to a 0.2 μm nitrocellulose blotting membrane (GE Healthcare Life Sciences, Chicago, USA), blocked with 5% skim milk in Tris-Buffered Saline (Biorad, Hercules, USA)-Tween 20 (1:1000) (Sigma-Aldrich, Burlington, USA) (TBS-T) for 1 h at room temperature (RT), and incubated overnight at 4°C with the primary antibodies: anti-mouse cleaved (CL) Gasdermin D (GSDMD) (1:1000, #10137, Cell Signaling Technologies, Danvers, USA), full GSDMD (1:1000, NBP233422, Novus Biologicals, Colorado, USA), CL caspase-1 (1:1000, PA599390, Invitrogen, ThermoFisher Scientific, Waltham, USA), CL caspase-3 (1:1000, #9661, Cell Signaling Technologies, Danvers, USA), histone 3 (1:3000, #9718, Cell Signaling Technologies, Danvers, USA) and α/β-tubulin (1:5000, #556321, Cell Signaling Technologies, Danvers, USA). Afterwards, membranes were washed 3 times with TBS-T for 5 min and incubated 1 h at RT with an anti-rabbit (1:10,000, #111-035-045, Jackson Immune Research, Philadelphia, USA) or anti-mouse (1:10,000, #115-035-062, Jackson Immune Research, Philadelphia, USA) Horseradish Peroxidase (HRP)-conjugate secondary antibody, washed with TBS-T and visualized with SuperSignal West Pico Chemiluminescent Substrate (#34580, ThermoFisher Scientific, Waltham, USA) using the ChemiDoc XRS+ imaging system (Biorad, Hercules, USA).

In vivo Experiments

Female 8 weeks old BALB/c mice, weighing 18–21 g, were obtained from Charles River Laboratories (Wilmington, USA). Mice were housed in a specific pathogen-free (SPF) environment with sterile food and water ad libitum with 12h light/12h dark cycles.

Mice were injected subcutaneously with 2.5×10^5 CT26-mCXCR4 cells. At day 9 post-injection, mice-bearing tumors (≈20 mm^3) were randomized into two groups (vehicle and treated). Vehicle group (n=6) was intravenously administered with 100 μL vehicle (166 mm $NaCO_3H$ pH 8.0), and treated animals (n=7) were administered with 0.5 mg/kg of T22-DITOX-H6 three times per week up to 6 doses. Animal body weight was registered once per week, whereas tumor size was measured with a caliper (tumor volume = $width^2 \times length/2$) every dose-day during the time course of the experiment. Mice were euthanized by cervical dislocation 72h after the last dose. Then, tumors and organs were collected for further analysis. Blood was extracted by intracardiac puncture for further liver and kidney function analysis

and placed in EDTA-tubes and centrifuged at 21,000 g for 10 min at 4 °C. Plasma was stored at −80 °C. Experimental procedures followed the ARRIVE Guidelines and were reviewed and approved by the Institutional Animal Care and Use Committee of the Sant Pau Research Institute and authorized by the Animal Experimental Committee of the local government authority (Generalitat de Catalunya, authorization No. 12001) in accordance with the Spanish Law (RD 53/2013) and European Directive 2010/63/EU. Procedures were performed at the Animal Experimentation Service, ISO 9001:2015 certified.

Flow Cytometry

In order to perform the flow cytometry experiment, spleen and bone marrow cells were isolated. Briefly, splenocytes were obtained homogenizing the spleen gently with a plunger on a 70 μm cell strainer, and then red blood cells were lysed incubating the cell suspension in Red Blood Cells lysis buffer (Invitrogen, ThermoFisher Scientific, Waltham, USA) for 5 min at RT. Finally, cell suspension was centrifuged at 500 *g* for 5 min at RT and cells resuspended in PBS-0.5% BSA for flow cytometry. On the other hand, bone marrow cells were harvested from mouse femurs. Shortly after, both femur ends were cut, with a 25-gauge syringe flushed out of the marrow. Then, the suspension was passed through a 70 μm cell strainer and red blood cells lysed using the buffer mentioned above. In the end, the cell suspension was centrifuged at 500 *g* for 5 min at RT, and cells resuspended in PBS-BSA 0.5% for flow cytometry.

To assess the mCXCR4 expression in splenocytes and bone marrow cells, as well as, in CT26-mCXCR4+ cells, 10^6 cells were stained with the antibodies: anti-mCXCR4 (#146505, Biolegend, San Diego, USA) and Viobility™ 488/520 Fixable Dye (#130-109-812, Miltenyi Biotec, Bergisch Gladbach, Germany).

Data experiment was analyzed with the MACSQuant® Analyzer 10 Flow Cytometer (Miltenyi Biotec, Bergisch Gladbach, Germany) and the software MACSQuantify ™ (Miltenyi Biotec, Bergisch Gladbach, Germany).

Sample Processing for Hematoxylin and Eosin (H&E), DAPI and Immunohistochemical (IHC) Staining

Paraffin-embedded organs were cut in 4 μm sections for staining. Organ sections were stained with H&E and analyzed by two independent observers. IHC staining was performed in a DAKO Autostainer Link 48 (Agilent Technologies, Santa Clara, USA) following the manufacturer's instructions. Firstly, sections were dewaxed, the antigen retrieval was made and finally stained in DAKO Autostainer Link 48 using the following primary antibodies: CXCR4 (1:1000, ab124824, Abcam, Cambridge, UK. Retrieval pH high, DAKO), Caspase-1 CL p20 (1:400, PA599390, Invitrogen, ThermoFisher Scientific, Waltham, USA. Retrieval pH low, DAKO), NLRP3 (1:300, ab270449, AdipoGen Life Sciences, San Diego, USA. Retrieval pH high, DAKO), IL-1β (1:500, ab205924, Abcam, Cambridge, UK. Retrieval pH low, DAKO), active caspase-3 (1:300, #559565, BD Bioscience, Franklin Lakes, USA. Retrieval pH low, DAKO), eosinophil peroxidase (EPX) (1:200, PA5-62200, ThermoFisher Scientific, Waltham, USA. Retrieval pH high, DAKO) and major basic protein (MBP) (1:50, MCA5751, Bio-Rad Laboratories, California, USA. Retrieval pH low, DAKO). IHC positive staining was identified and quantified with the SlideViewer software (3DHistech, Budapest, Hungary). DAPI staining was performed as follows, paraffin-embedded sections were dewaxed, rehydrated, and permeabilized with PBS-10% Triton X-100. Then, sections were stained with DAPI mounting medium (ProLongTM Gold Antifade Mountant, Thermo Fisher Scientific, Waltham, USA) and incubated at 4 °C overnight. DAPI evaluation was carried out to detect condensed DNA as a surrogate of dead cells. DAPI quantification was performed by counting the number of condensed nuclei per mm^2.

Plasma Analysis

In order to evaluate the derived toxicity at hepatic and renal level from the T22-DITOX-H6 treatment in immunocompetent mice, aspartate transaminase (AST) and alanine transaminase (ALT) enzyme activities, in addition to albumin, creatinine and uric acid levels, were measured in plasma samples obtained at the end of the experiment with commercial kits (Roche Diagnostics, Basel, Switzerland) adapted for a COBAS 6000 autoanalyzer (Roche Diagnostics, Basel, Switzerland).

Statistical Analyses

Data appears as mean ± standard error of the mean (SEM). Statistical analyses were performed using GraphPad Prism 8 software (GraphPad Software, San Diego, USA). Results were analyzed by Mann–Whitney *U*-test and 2-way ANOVA tests. Differences were considered statistically significant when p-values < 0.05. All experiments were performed at least in triplicates.

Results

T22-DITOX-H6 Has a Potent mCXCR4-Dependent Cytotoxic Effect in vitro

Membrane mCXCR4 expression in the mouse colorectal tumor-derived cell-line CT26 was evaluated using flow cytometry. We found that 2.81±0.95% of the parental cells expressed CXCR4 (Figure S1). To establish a proper model for studying the antitumor effect of the CXCR4-targeted nanotoxin T22-DITOX-H6 in an immunocompetent model, CT26 cells were transduced with mCXCR4 and selected by their mCXCR4 membrane expression, obtaining a cell line with the 95.25±2.07% of cells expressing CXCR4 at the membrane (CT26-mCXCR4). Our data indicated that T22-DITOX-H6 efficiently decreased the viability of CT26-mCXCR4 (IC50 = 0.254 ± 0.079 nM), while the parental cells (CT26-Par) did not exhibit cytotoxicity upon treatment (Figure 1b).

As expected, the blockage of the receptor using a CXCR4 antagonist (AMD3100) before nanotoxin exposure completely prevented cell death triggered by T22-DITOX-H6 (Figure 1c). These results suggest that mCXCR4 expression in the cell membrane is required for T22-DITOX-H6 cytotoxicity.

The observed cell death was due to caspase activation, since pretreatment with a pan-caspase inhibitor, z-VAD, blocked the cytotoxic effect of the nanotoxin (Figure 1d). Two main cell death mechanisms are triggered by caspases, namely apoptosis and pyroptosis. Upon treatment, no cleavage of caspase-3 was observed, whereas the molecular markers of the canonical pyroptotic pathway (cleaved caspase-1 and cleaved N-terminal Gasdermin D) increased upon nanotoxin exposure, suggesting that T22-DITOX-H6 activates pyroptosis in this cell line (Figure 1e).

During pyroptosis, cellular contents are released into the extracellular media. Therefore, we quantified lactate dehydrogenase (LDH) in the CT26-mCXCR4 cell culture supernatant after T22-DITOX-H6 exposure to confirm the activation of lytic death. In agreement with pyroptosis activation, we detected a statistically significant enhancement in the supernatant LDH at 48 h that was impaired by the use of CXCR4 antagonist or a pan-caspase inhibitor (Figure 1f).

Repeated Doses of T22-DITOX-H6 Exhibited Potent Antitumor Effects in a Mouse Colorectal Tumor Model

Considering the potent cytotoxic effect of T22-DITOX-H6 showed in the murine colon carcinoma cell line CT26-mCXCR4, we decided to evaluate its antitumor effect in vivo. Therefore, a subcutaneous syngeneic mouse model was developed. On day 9 after subcutaneous cell implantation, when tumors were approximately 20 mm^3, animals were randomized and intravenously administered with vehicle or 0.5 mg/kg T22-DITOX-H6 three times per week up to six doses. Animal body weight was recorded once per week. Animals were euthanized 72 h after the final dose. At this point, the tumors were measured (Figure 2a) and collected for further analyses along with the liver, kidney, spleen, bone marrow, and plasma.

As directed by these findings, the ex vivo tumor size at the end of the experiment was significantly larger in vehicle-treated animals than in nanotoxin-treated mice (Figure 2b). In agreement with this, the tumor growth rate was different between the two groups (Figure 2c). Next, we evaluated cell death within the tumor using DAPI staining to quantify nuclei with highly condensed chromatin as a surrogate of cell death (Figure 2d). T22-DITOX-H6 treated tumors showed a 3-fold increase in the number of dead cells per mm^2 compared with the vehicle group (Figure 2e).

T22-DITOX-H6-Induced Pyroptosis Stimulates Innate Immune Cell Infiltration in vivo

Next, we validated the in vitro observations regarding the cell death mechanism triggered by T22-DITOX-H6. Thus, immunohistochemistry was performed for NLRP3, cleaved caspase-1, IL-1β, and cleaved caspase-3. Quantification of protein expression revealed that NLRP3, cleaved caspase-1 and IL-1β were nearly three times more expressed in tumors from mice treated with T22-DITOX-H6 than in vehicle-treated mice. In the case of cleaved caspase-3, no differences in

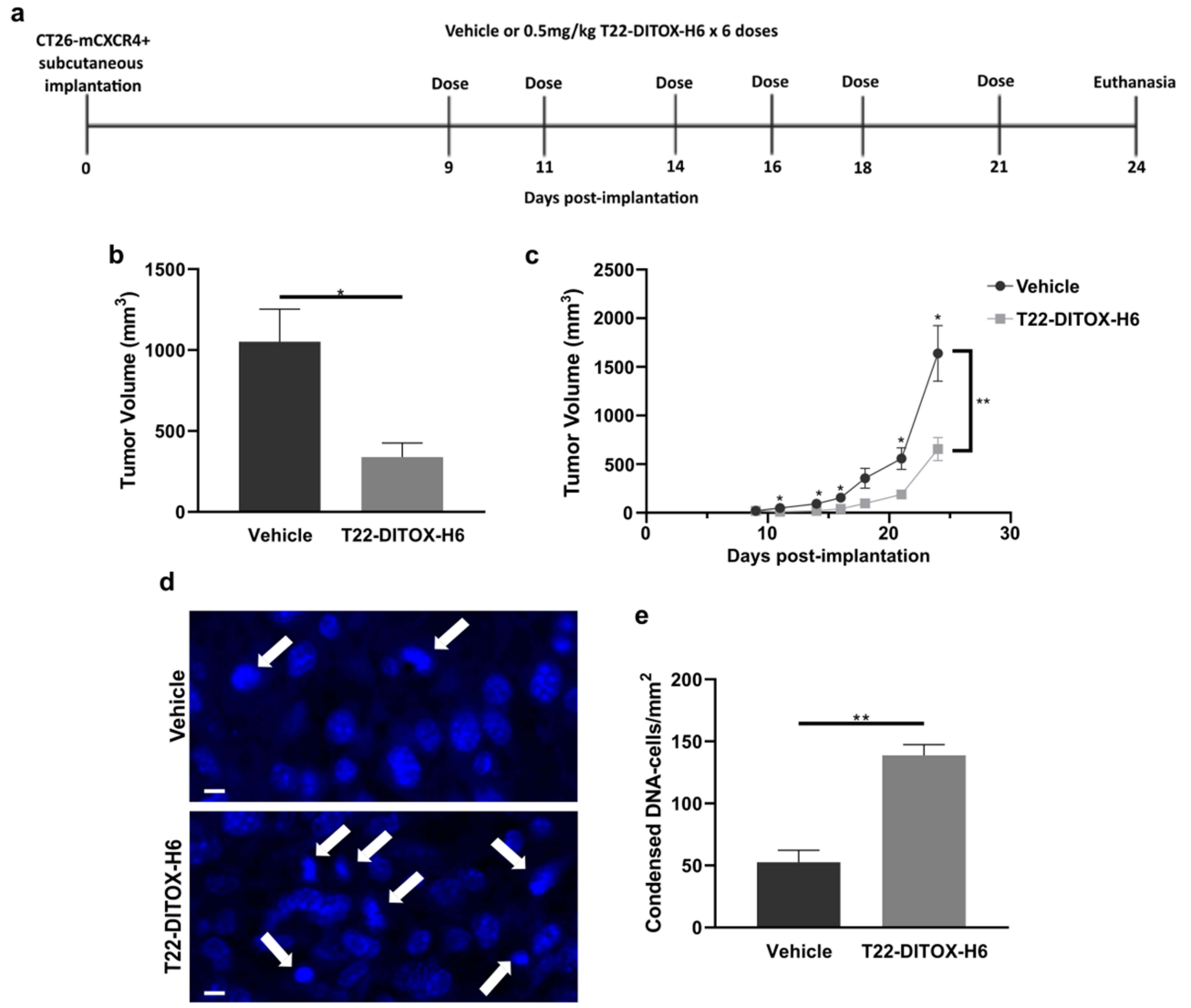

Figure 2 T22-DITOX-H6 antitumor effects in a CT26-mCXCR4+ subcutaneous mouse model. (**a**) Schematic representation of the experimental timeline of the study. (**b**) Final tumor volume measured ex vivo at the end of the experiment. (n=13) (**c**) Evolution of the tumor volume in each group (Vehicle and T22-DITOX-H6) during the time course of the experiment. (n=13) (**d**) Representative images of tumor sections stained with DAPI (blue) to detect condensed DNA as a surrogate of dead cells. Arrows indicate condensed DNA-cells. (**e**) Quantification of the number of tumor cells with condensed DNA per mm2. Scale bars = 50 μm and 10 μm (zoom in). (n=12) Error bars indicate ± SEM. *$p<0.05$; **$p<0.01$.

expression were observed between groups (Figure 3). Our results confirmed that T22-DITOX-H6 nanotoxin triggers pyroptosis in vivo through the canonical pathway.[27]

Recently, eosinophils have been described as an immune population with anti-tumorigenic roles in CRC, and their presence within the tumor microenvironment has been associated with improved overall survival.[17–20,22,28] Moreover, bacterial pathogens that penetrate the intestine mucosal barrier display DAMPs that are sensed by Toll-like and RIG-I-like receptors by the eosinophil residents in the lamina propia, which release cytotoxic granules that kill the infected cells to maintain tissue homeostasis.[15]

On this basis, we evaluated whether the inflammation generated by the local pyroptosis induced by T22-DITOX-H6 similarly recruits eosinophils to the CRC tumor to kill epithelial cancer cells.[15] For this, we performed immunochemistry in the tumors regarding the presence of eosinophils by detecting EPX (Figure 4a and b) and MBP (Figure 4c and d). Both proteins are found in the granules of eosinophils and exhibit potent cytotoxic properties when released to the extracellular

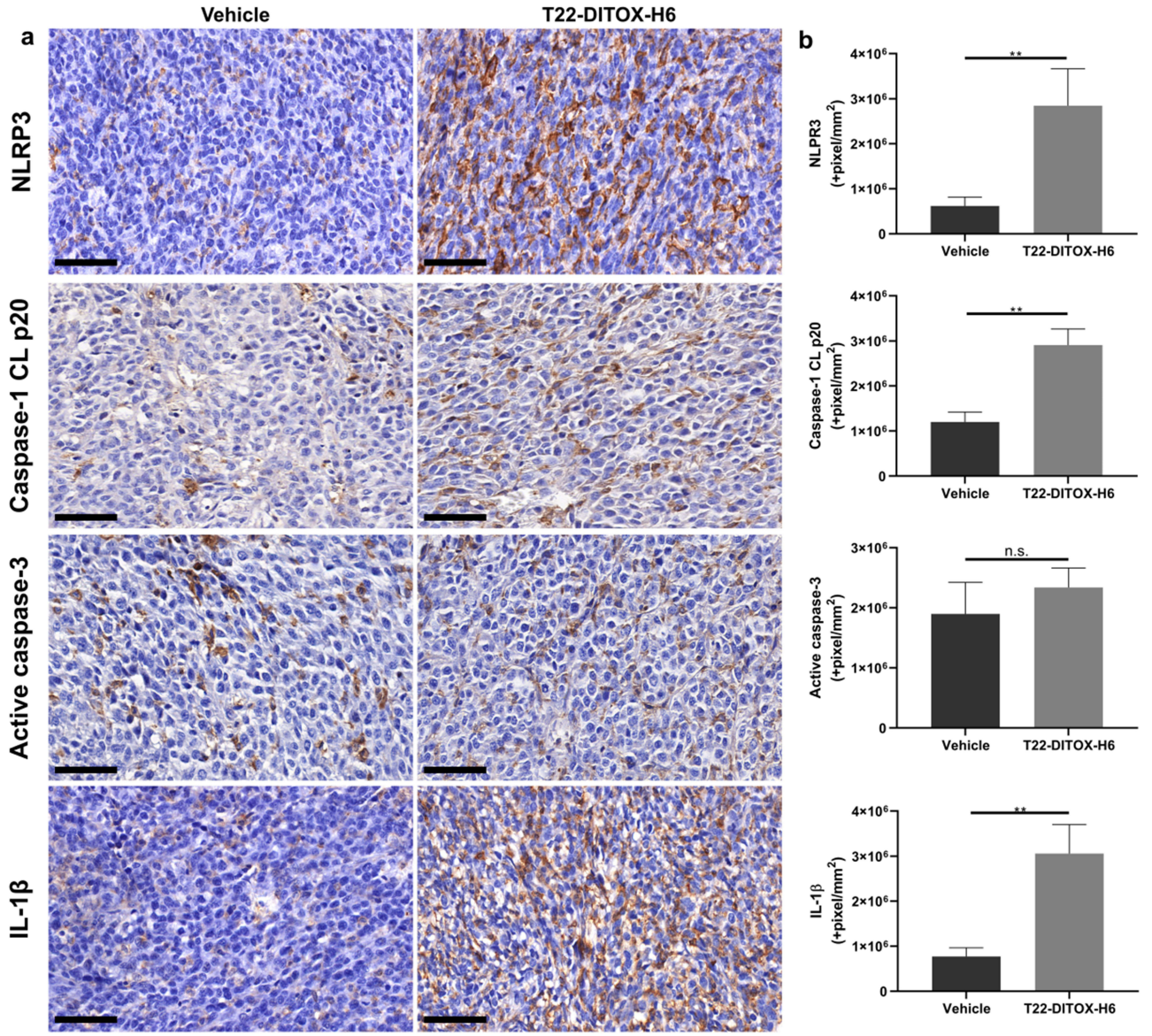

Figure 3 Immunodetection of NLRP3, Caspase-1, Caspase-3, and IL-1β in CT26-mCXCR4+ subcutaneous tumors upon T22-DITOX-H6 treatment. Tumor sections from mice treated with T22-DITOX-H6 or vehicle were stained by immunohistochemistry (IHC) for NLRP3, cleaved (CL) caspase-1 p20, CL caspase-3, and IL-1β. (**a**) Representative IHC images. (**b**) Quantification of stained positive pixels per mm^2 for NLRP3, CL caspase-1 p20, CL caspase-3, and IL-1β. (n=12) Error bars indicate ±SEM. Scale bars = 50 μm. $^{**}p<0.01$.

space.[14,16] The eosinophil staining per mm^2 in T22-DITOX-H6 treated tumors was found to be 5-fold increase compared to vehicle-treated tumors, looking at both components (Figure 4b and d).

In a closer look, it can be observed that degranulation of eosinophils leads to secretion of EPX and MBP that surround cancer cells (Figure 4e and f) suggesting eosinophils recruited to the tumor upon T22-DITOX-H6 treatment participate in the destruction of tumor cells. Therefore, pyroptosis activation stimulated by the nanotoxin developed by us triggered eosinophil recruitment to the tumor microenvironment (Figure 4).

Cell Death Is Triggered in CXCR4-Overexpressing Tumor Cells but Not in Healthy Organs

Cells from the spleen and bone marrow were isolated from wild-type mice and analyzed using flow cytometry (Figure S2). CXCR4 expression in the spleen and bone marrow was lower than that in tumor tissue (Figure S2). The percentage of cells with membrane expression of CXCR4 was 14.04% and 27.56% in splenocytes and bone marrow, respectively (Figure S2b),

https://doi.org/10.2147/IJN.S499192

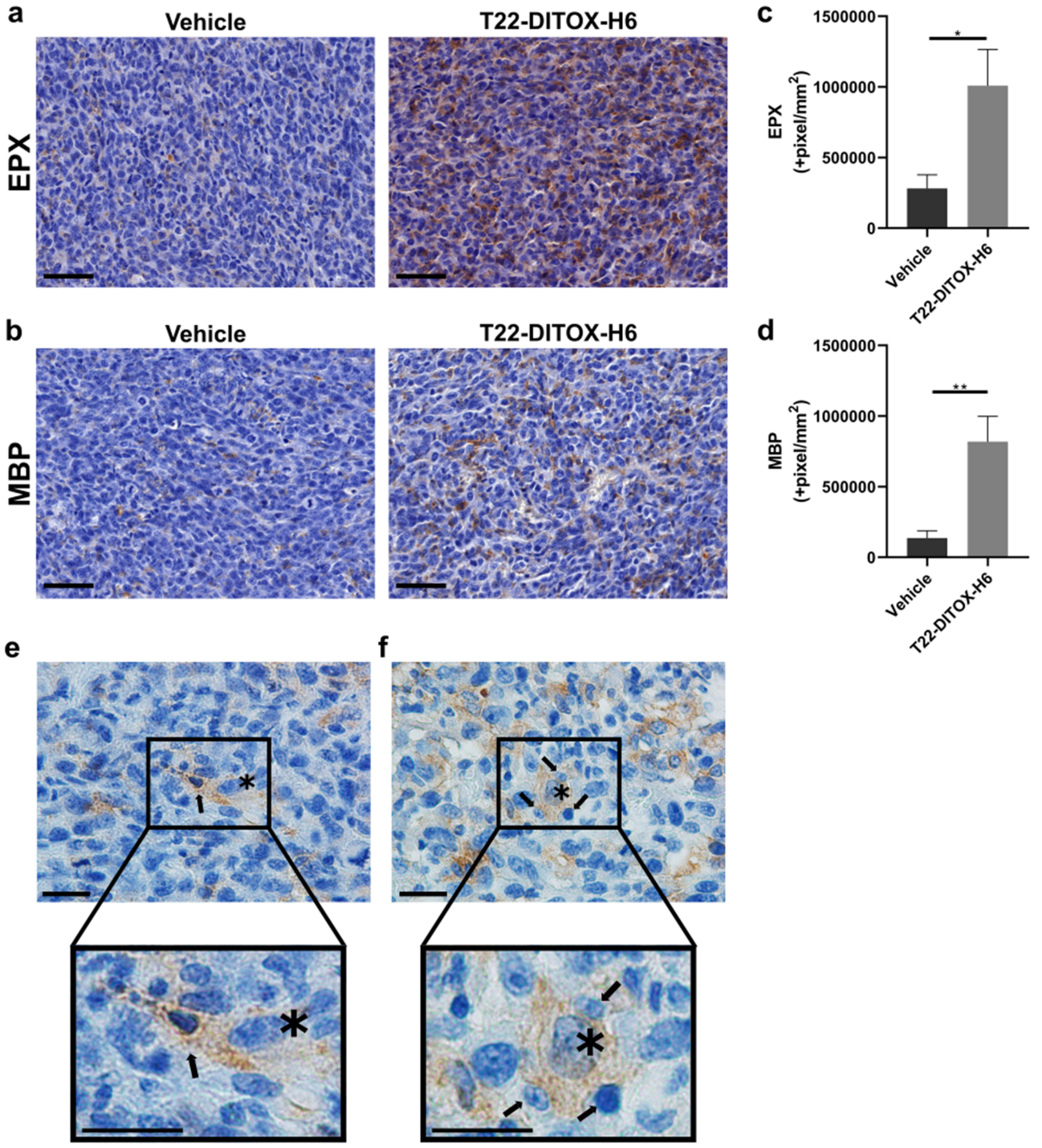

Figure 4 Eosinophils are recruited to the tumor after repeated doses of T22-DITOX-H6. Eosinophil cytotoxic proteins, (**a**) eosinophil peroxidase-EPX and (**b**) major basic protein-MBP, were detected in tumor sections from both experimental groups. (**c** and **d**) Positive pixels per mm^2 of tumor tissue were quantified and compared between the groups. (n=12) (**e** and **f**) Representative IHC image of tumors treated with T22-DITOX-H6 showing tumor cell (asterisk) being attacked by eosinophil (arrow) in (**e**) EPX and (**f**) MBP staining. Error bars indicate ±SEM. **p*<0.05; ***p*<0.01. Scale bars = 50 μm (**a, c**); 20 μm (**e** and **f**).

whereas that of CT26-mCXCR4 was 96.46%. CXCR4 expression was also assessed in these organs using immunohistochemistry, and the same result was obtained (Figure S2c).

Interestingly, when analyzing toxicity in the spleen and bone marrow, no morphological differences in tissue structure were detected between the vehicle- and nanotoxin-treated groups (Figure 5a). Moreover, the number of dead cells per mm^2 was

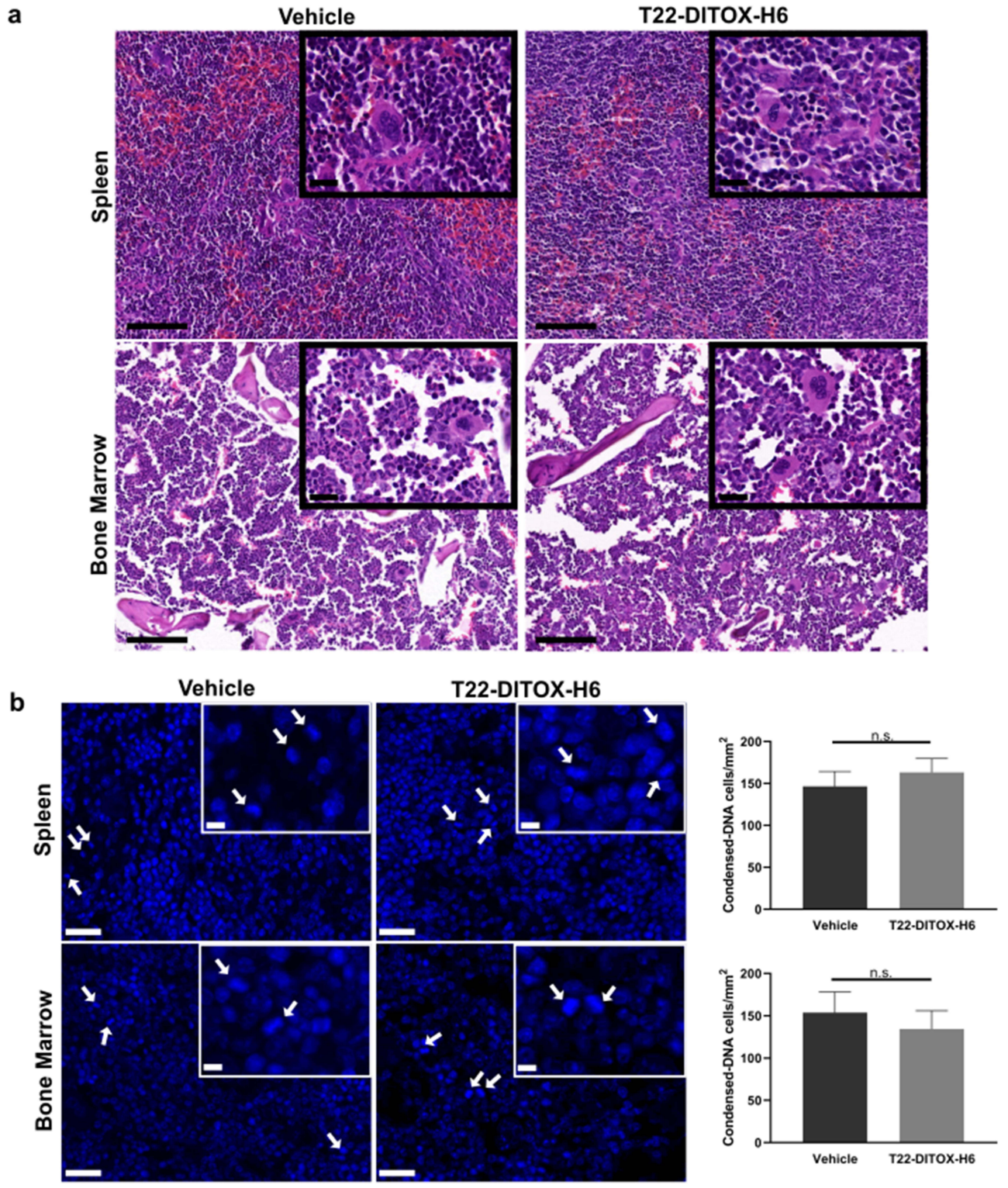

Figure 5 On-target toxicity of T22-DITOX-H6 in an immunocompetent mouse model. (**a**) Histopathological analysis by H&E staining of the spleen and bone marrow, both non-tumor CXCR4-expressing tissues, from vehicle and T22-DITOX-H6 treated animals. (**b**) On-target toxicity was assessed by the detection of dead cells (condensed DNA, white arrows) in spleen (n=13) and bone marrow (n=7) sections stained with DAPI. (**a**) Scale bars = 100 μm and 20 μm (zoom in). (**b**) Scale bars = 50 μm and 5 μm (zoom in). Error bars indicate ±SEM.

https://doi.org/10.2147/IJN.S499192

similar in the organs of both groups (Figure 5b), indicating that the nanotoxin did not exert cytotoxic effects on non-tumor cells. Finally, systemic toxicity, regardless of mCXCR4 expression, was not observed. In addition, mouse plasma was analyzed at the final point to detect alterations in renal and hepatic functions. The aspartate aminotransferase (AST), alanine transaminase (ALT), creatinine, albumin, and uric acid levels did not differ between the groups (Figure S3a), confirming the absence of liver or kidney failure due to treatment. As expected, the histology of the mentioned organs was normal with conserved structures (Figure S3b). Finally, the mice did not exhibit any discomfort or weight loss throughout the experiment (Figure S3c).

Discussion

Here, we describe that repeated intravenous administration of the multivalent nanotoxin T22-DITOX-H6, which targets CT26-mCXCR4 overexpressing (CXCR4+) cancer cells, induces potent antitumor activity in an immunocompetent CRC model, without systemic toxicity. These findings confirm that the multiple T22 ligands displayed by this nanotoxin are able to selectively internalize in cancer target cells to reach their cytosol and deliver its exotoxin domain to inhibit translation.[10] In turn, this inhibition induces pyroptosis, the exact cell death mechanism that we previously reported in immunosuppressed models.[8,9] In addition, we found, for the first time, that the induction of pyroptosis in an immunocompetent CRC model induces local inflammation and activation of the host immune cells in tumor tissue, which involves eosinophil infiltration in tumor tissue and degranulation associated with tumor growth blockade.

First, we show that T22-DITOX-H6 displays a potent mCXCR4-dependent cytotoxic effect in a cultured CT26-mCXCR4+ murine CRC cell line, with an IC50 in the low nanomolar range (0.254 ± 0.079 nM). In addition, cell death induction is mediated by caspases, as a pan-caspase inhibitor reverses cytotoxicity. We also determined that the cell death mechanism triggered by T22-DITOX-H6 is not apoptosis, since exposure to the nanotoxin does not activate caspase-3. Instead, it triggers lytic cell death, as observed by LDH released in the supernatant. This lytic death is mediated by pyroptosis, which cleaves caspase-1, which, once activated, cleaves GSDMD, allowing its N-terminal domain to oligomerize to form pores in the cell membrane to free the target cancer cell content to the extracellular space, as reported previously.[29] Additionally, the cytotoxicity was reversed by prior exposure to the CXCR4 inhibitor AMD3100, demonstrating that cell death is dependent on CXCR4.

In agreement with the in vitro observations, in a CXCR4+ CRC mouse model, repeated doses of T22-DITOX-H6 in tumor-bearing mice exhibited a potent antitumor effect (Figure 2b). The mechanism of action of the nanotoxin encompasses CXCR4-dependent internalization, furin cleavage to separate the catalytic domain from the targeting peptide and the translocation domain, which facilitate endosomal escape to avoid lysosomal degradation and reach the cytosol of targeted cancer epithelial cells, where it inhibits protein translation and induces cell death.[10] In this study, we demonstrated that T22-DITOX-H6 administration induces pyroptosis through its canonical pathway in vivo, a finding confirmed by immunodetection of the tumor tissue, the mediator of inflammation, NLRP3, the cleavage of the inflammation-mediated caspase-1, and a significant release of IL-1β, a marker of GSDMD-dependent pyroptosis,[27] discarding apoptotic cell death, since caspase-3 was not activated (Figure 3).

Pyroptosis has been described as a highly immunogenic type of cell death.[13] In line with this, our data show that activation of pyroptosis within the tumor stimulates the recruitment of host immune cells to fight against tumor cells. Specifically, our results indicate that upon T22-DITOX-H6-there is an increase in EPX and MBP proteins (Figure 4), both cytotoxic enzymes produced and released exclusively by eosinophils,[14] suggesting that DAMPs released following pyroptosis activation stimulates eosinophil recruitment to the tumor microenvironment. Subsequently, EPX and MBP granules are released into the extracellular space to kill cancer cells. Our findings suggest that T22-DITOX-H6 not only exerts its cytotoxic effect by eliminating CXCR4+ cells but is also a potent stimulator of eosinophil infiltration in the tumor tissue due to pyroptosis activation.

This finding also agrees with the display of tumor-associated tissue eosinophilia (TATE) in patients with CRC as an independent variable of good prognosis.[30–35] The infiltration and activation of eosinophils into the tissues after DAMPs or alarmins injection have been previously reported in other pathologies such as asthma, eosinophilic esophagitis, and bacterial infections.[15,31,36,37] Our observations in cancer tissue mimic the response to bacterial infection, which is mediated by eosinophil infiltration in infected tissues to provide protection against bacterial invasion,[38] which is able to induce

pyroptosis in epithelial infected cells, followed by the engagement of host eosinophils as an immune response to the infection.[16,39,40]

On this basis, we believe that the degranulation and release of EPX and MBP observed in our antitumor experiments is the mechanism by which eosinophils kill cancer cells. Other authors have found that cultured colon carcinoma cells require direct contact with eosinophils to induce cytotoxicity in cancer cells by ECP, EDN, TNF-α, and granzyme A.[41] Similarly, eosinophil lysates are cytotoxic to B16 melanoma cells.[42] Moreover, in vivo, the degranulation of tumor-infiltrated eosinophils is essential to induce cytotoxicity against CRC cells to induce an antitumor effect.[20,22,28] Moreover, the killing of cancer cells through the recruitment of eosinophils in the local tumor, after T22-DITOX-H6-induced pyroptosis, mimics the recruitment of resident eosinophils to kill the inflamed intestinal epithelial induced by intruding bacteria.[15]

In summary, the development of the T22-DITOX-H6 natotoxin based on pyroptotic inflammation, leading to eosinophil recruitment and activation, is associated with tumor growth inhibition. This, novel approach to the large effort done by the pharmaceutical industry in developing pro-inflammatory agonists of STING, NLRP3 or RIGI, already in clinical trials, that also focuses in activating the innate immune system to kill cancer cells.[43,44]

Notably, the exotoxin domain incorporated in T22-DITOX-H6 has the same amino acid sequence as the domain included in previously developed immunotoxins (ITs) which consist of the diphtheria toxin linked to a targeted monoclonal antibody. This domain has been deimmunized by mutagenizing specific epitopes of T and B lymphocytes to avoid antibody-mediated neutralization of this cytotoxic domain.[45] The FDA approved two ITs, Tagraxofusp-erzs, targeting IL-3R, and denileukin diftitox, targeting IL-2R, and also DAB486IL-2 and A-dmDT390-bisFV now in clinical trials are designed to treat diverse but minority hematological malignancies.[46] ITs have been shown to be highly cytotoxic, showing a potent anticancer effect; however, they induce severe adverse effects induced by capillary leak syndrome (CLS), which caused the withdrawal of denileukin diftitox from the market, as well as additional side effects, such as ascites, hypoalbuminemia, increased creatinine, and renal insufficiency, associated with hemolysis and thrombocytopenia, and an increase in hepatic transaminases and liver injury.

In contrast, we did not observe any alterations in plasma albumin, hepatic transaminase levels, renal injury markers, or histological alterations in the liver or kidney, highlighting the present nanotoxin as a safe therapeutic agent for cancer treatment. More importantly, we did not observe on-target toxicity (CXCR4-expressing tissues: bone marrow (BM) and spleen (SP)) after nanotoxin dosage; thus, BM and SP in treated animals showed no histopathological alteration, along with the same (low) number of dead cells, in the microscopic field, as the untreated control tissues. This phenomenon occurs due to the multivalence of the T22-DITOX-H6 nanotoxin, which triggers superselectivity towards overexpressing-CXCR4+ CRC cells, achieving local delivery of the nanotoxin in tumor tissues, which improves the anticancer effect while drastically reducing on-target and off-target toxicity. Consistent with our argument, enhancement of cell death was observed in tissues with a high CXCR4 H-Score (tumor) rather than lower ones (bone marrow or spleen), which agrees with previous regarding the biodistribution of the nanocarrier, where we observed that the uptake of CXCR4-targeted nanoparticle reaches 70–80% of the administered dose in tumor tissue in different cancer models, meaning that only a small amount could reach normal tissues, a quantity that does not produce any toxicity.[47–50] In contrast, for the described ITs, only a small amount of the injected dose (<1%) reaches the tumor, limiting their clinical translation due to toxicity.[51] Consistently, antibody-drug conjugates (ADCs) reach a tumor uptake of 0.1%,[52] because of their pharmacokinetics that are determined by the antibody rather than the attached cytotoxic drug.

Conclusion

The multivalent nanotoxin T22-DITOX-H6 selectively delivers the cytotoxic diphtheria exotoxin to CXCR4+ cancer cells in tumor tissue without affecting non-tumor tissues, thereby widening the nanotoxin therapeutic window. The T22-DITOX-H6 mechanism of action leads to local tumor pyroptosis and inflammation, which attracts eosinophils to the tumor site and eliminates cancer cells through the release of cytotoxic granules. Our results support the engagement of the eosinophil effector function as an effective therapeutic approach against colorectal cancer.

Abbreviations

ADC, Antibody-drug conjugate; ALT, Alanine aminotransferase; AST, Aspartate aminotransferase; CRC, Colorectal cancer; CL, cleaved; CSC, Cancer stem cells; DAMPs, damage-associated molecular patterns; EPX, Eosinophils peroxidase; FDA, Food and drug administration; GSDMD, Gasdermin D; H&E, Hematoxylin and eosin; IHC, Immunohistochemistry; IT, Immunotoxins; LDH, Lactate dehydrogenase; MBP, Major basic protein; NS, No significant; SEM, Standard Error of the Media; TATE, Tumor-associated tissue eosinophilia.

Acknowledgments

This work was supported by Instituto de Salud Carlos III (PI21/00150, PI18/00650, EU COST Action CA17140 and CA21135 to R.M.; PI20/00400 and PI23/00318 to U·U.) co-funded by European Regional Development Fund (ERDF, a way to make Europe); Agencia Estatal de Investigacion (AEI) and Fondo Europeo de Desarrollo Regional (FEDER) (grant PID2020-116174RB-I00) to A.V.; (grant PID2019-105416RB-I00/AEI/10.13039/501100011033 and PDC2022-133858-I00) to E.V.; CIBER-BBN (CB06/01/1031 and 4NanoMets to R.M., VENOM4CANCER to A.V., NANOREMOTE to E.V. and NANOSCAPE to U·U.); AGAUR (2017-SGR-865, 2021-SGR-01140 to R.M. and 2017SGR-229 to A.V.); Josep Carreras Leukemia Research Institute (P/AG to I. C.); L.A-C and U.U. are supported by Miguel Servet fellowship (CP24/00111 and CP19/00028) and L.M.C. was supported by a predoctoral fellowship (FI19/00148) all from Instituto de Salud Carlos III co-funded by European Social Fund (ESF investing in your future); L.A.C was supported by a postdoctoral fellowship from AECC (POSTD20070ALBA, Spanish Association Against Cancer, Spain). E.V.D was supported by a predoctoral fellowship from Ministerio de Ciencia e Innovación, Spain (FPU18/04615). We are also indebted to CERCA (Research Centres of Catalonia). The histological and toxicity studies have been performed in the CIBER-BBN Nanotoxicology Unit 18 (http://www.nanbiosis.es/portfolio/u18-nanotoxicology-unit/), ICTS NANBIOSIS (entry accesses 2958 and 3291). Protein production has been partially performed by the ICTS "NANBIOSIS", more specifically by the Protein Production Platform of CIBER-BBN/IBB (http://www.nanbiosis.es/unit/u1-protein-production-platform-ppp/).

Disclosure

The authors declare the following financial interests/personal relationships which may be considered as potential competing interests: E.V., R.M. and A.V. are co-founders of Nanoligent, a company devoted to develop anticancer drugs based on proteins. U.U., E.V., A.V., R.M. and I.C. are cited as inventors in a patent application covering the therapeutic use of T22 (EP12704711.6) and nanostructures proteins (EP18726744.8). In addition, R.M. has patents PCT/EP2018/061732 and PCT/EP2012/050513 licensed to Nanoligent. U.U and I.C are scientific advisors of Nanoligent. All other authors report no conflicts of interest in this work.

References

1. Cervantes A, Prager GW. FOLFOXIRI plus bevacizumab as standard of care for first-line treatment in patients with advanced colon cancer. *ESMO open*. 2023;8(2):100883. doi:10.1016/J.ESMOOP.2023.100883
2. Qian S, Wei Z, Yang W, Huang J, Yang Y, Wang J. The role of BCL-2 family proteins in regulating apoptosis and cancer therapy. *Front Oncol*. 2022;12. doi:10.3389/FONC.2022.985363
3. Mohammad RM, Muqbil I, Lowe L, et al. Broad targeting of resistance to apoptosis in cancer. *Semin Cancer Biol*. 2015;35Suppl(0):S78–S103. doi:10.1016/J.SEMCANCER.2015.03.001.
4. Safa AR. Resistance to cell death and its modulation in cancer stem cells. *Crit Rev Oncog*. 2016;21(3–4):203–219. doi:10.1615/CRITREVONCOG.2016016976
5. Schuurhuizen CSEW, Braamse AMJ, Konings IRHM, et al. Does severe toxicity affect global quality of life in patients with metastatic colorectal cancer during palliative systemic treatment? A systematic review. *Ann Oncol off J Eur Soc Med Oncol*. 2017;28(3):478–486. doi:10.1093/ANNONC/MDW617
6. Casak SJ, Marcus L, Fashoyin-Aje L, et al. FDA approval summary: pembrolizumab for the first-line treatment of patients with MSI-H/dMMR advanced unresectable or metastatic colorectal carcinoma. *Clin Cancer Res*. 2021;27(17):4680–4684. doi:10.1158/1078-0432.CCR-21-0557/672273/AM/FDA-APPROVAL-SUMMARY-PEMBROLIZUMAB-FOR-THE-FIRST
7. Shek D, Akhuba L, Carlino MS, et al. Immune-checkpoint inhibitors for metastatic colorectal cancer: a systematic review of clinical outcomes. *Cancers (Basel)*. 2021;13(17):4345. doi:10.3390/CANCERS13174345
8. Serna N, Álamo P, Ramesh P, et al. Nanostructured toxins for the selective destruction of drug-resistant human CXCR4+ colorectal cancer stem cells. *J Control Release*. 2020;320(August 2019):96–104. doi:10.1016/j.jconrel.2020.01.019
9. Sala R, Rioja-Blanco E, Serna N, et al. GSDMD-dependent pyroptotic induction by a multivalent CXCR4-targeted nanotoxin blocks colorectal cancer metastases. *Drug Deliv*. 2022;29(1):1384–1397. doi:10.1080/10717544.2022.2069302
10. Sánchez-García L, Serna N, Álamo P, et al. Self-assembling toxin-based nanoparticles as self-delivered antitumoral drugs. *J Control Release*. 2018;274(January):81–92. doi:10.1016/j.jconrel.2018.01.031

11. Chatterjee S, Behnam Azad B, Nimmagadda S. The intricate role of CXCR4 in cancer. *Adv Cancer Res*. 2014;124:31–82. doi:10.1016/B978-0-12-411638-2.00002-1
12. Domanska UM, Kruizinga RC, Nagengast WB, et al. A review on CXCR4/CXCL12 axis in oncology: no place to hide. *Eur J Cancer*. 2013;49(1):219–230. doi:10.1016/J.EJCA.2012.05.005
13. Legrand AJ, Konstantinou M, Goode EF, Meier P. The diversific ation of cell death and immunity: memento mori. *Mol Cell*. 2019;76(2):232–242. doi:10.1016/J.MOLCEL.2019.09.006
14. Acharya KR, Ackerman SJ. Eosinophil granule proteins: form and function. *J Biol Chem*. 2014;289(25):17406–17415. doi:10.1074/JBC.R113.546218
15. Gurtner A, Gonzalez-Perez I, Arnold IC. Intestinal eosinophils, homeostasis and response to bacterial intrusion. *Semin Immunopathol*. 2021;43(3):295–306. doi:10.1007/S00281-021-00856-X
16. Gaur P, Zaffran I, George T, Rahimli Alekberli F, Ben-Zimra M, Levi-Schaffer F. The regulatory role of eosinophils in viral, bacterial, and fungal infections. *Clin Exp Immunol*. 2022;209(1):72–82. doi:10.1093/CEI/UXAC038
17. Nielsen HJ, Hansen U, Christensen IJ, Reimert CM, Brünner N, Moesgaard F. Independent prognostic value of eosinophil and mast cell infiltration in colorectal cancer tissue. *J Pathol*. 1999;189(4):487–495. doi:10.1002/(SICI)1096-9896(199912)189:4.
18. Davis BP, Rothenberg ME. Eosinophils and cancer. *Cancer Immunol Res*. 2014;2(1):1–8. doi:10.1158/2326-6066.CIR-13-0196
19. Prizment AE, Vierkant RA, Smyrk TC, et al. Tumor eosinophil infiltration and improved survival of colorectal cancer patients: Iowa Women's Health Study. *Mod Pathol*. 2016;29(5):516–527. doi:10.1038/MODPATHOL.2016.42
20. Fernández-Aceñero MJ, Galindo-Gallego M, Sanz J, Aljama A. Prognostic influence of tumor-associated eosinophilic infiltrate in colorectal carcinoma. *Cancer*. 2000;88(7):1544–1548. doi:10.1002/(sici)1097-0142(20000401)88:7<1544::aid-cncr7>3.0.co;2-s
21. Shunyakov L, Ryan CK, Sahasrabudhe DM, Khorana AA. The influence of host response on colorectal cancer prognosis. *Clin Colorectal Cancer*. 2004;4(1):38–45. doi:10.3816/CCC.2004.N.008
22. Pretlow TP, Keith EF, Cryar AK, et al. Eosinophil infiltration of human colonic carcinomas as a prognostic indicator. *Cancer Res*. 1983;43(6):2997–3000.
23. Medina-Gutiérrez E, García-León A, Gallardo A, et al. Potent anticancer activity of CXCR4-targeted nanostructured toxins in aggressive endometrial cancer models. *Cancers (Basel)*. 2023;15(1). doi:10.3390/cancers15010085
24. Falgàs A, Garcia-León A, Núñez Y, et al. A diphtheria toxin-based nanoparticle achieves specific cytotoxic effect on CXCR4+ lymphoma cells without toxicity in immunocompromised and immunocompetent mice. *Biomed Pharmacother*. 2022;150. doi:10.1016/J.BIOPHA.2022.112940.
25. Rioja-Blanco E, Arroyo-Solera I, Álamo P, et al. CXCR4-targeted nanotoxins induce GSDME-dependent pyroptosis in head and neck squamous cell carcinoma. *J Exp Clin Cancer Res*. 2022;41(1):49. doi:10.1186/s13046-022-02267-8
26. Pallarès V, Núñez Y, Sánchez-García L, et al. Antineoplastic effect of a diphtheria toxin-based nanoparticle targeting acute myeloid leukemia cells overexpressing CXCR4. *J Control Release*. 2021;335:117–129. doi:10.1016/J.JCONREL.2021.05.014
27. Liu Y, Pan R, Ouyang Y, et al. Pyroptosis in health and disease: mechanisms, regulation and clinical perspective. *Signal Transduct Target Ther*. 2024;9(1):245. doi:10.1038/S41392-024-01958-2
28. Reichman H, Itan M, Rozenberg P, et al. Activated eosinophils exert antitumorigenic activities in colorectal cancer. *Cancer Immunol Res*. 2019;7(3):388–400. doi:10.1158/2326-6066.CIR-18-0494
29. Xia S, Zhang Z, Magupalli VG, et al. Gasdermin D pore structure reveals preferential release of mature interleukin-1. *Nature*. 2021;593:7860):607–611. doi:10.1038/S41586-021-03478-3
30. Fettrelet T, Gigon L, Karaulov A, Yousefi S, Simon HU. The Enigma of Eosinophil Degranulation. *Int J mol Sci*. 2021;22(13):7091. doi:10.3390/IJMS22137091
31. Rothenberg ME. Eosinophilic gastrointestinal disorders (EGID). *J Allergy Clin Immunol*. 2004;113(1):11–28. doi:10.1016/j.jaci.2003.10.047
32. Ono Y, Ozawa M, Tamura Y, et al. Tumor-associated tissue eosinophilia of penile cancer. *Int J Urol*. 2002;9(2):82–87. doi:10.1046/J.1442-2042.2002.00424.X
33. Luna-Moré S, Florez P, Ayala A, Diaz F, Santos A. Neutral and acid mucins and eosinophil and argyrophil crystalloids in carcinoma and atypical adenomatous hyperplasia of the prostate. *Pathol Res Pract*. 1997;193(4):291–298. doi:10.1016/S0344-0338(97)80006-4
34. Fujii M, Yamashita T, Ishiguro R, Tashiro M, Kameyama K. Significance of epidermal growth factor receptor and tumor associated tissue eosinophilia in the prognosis of patients with nasopharyngeal carcinoma. *Auris Nasus Larynx*. 2002;29(2):175–181. doi:10.1016/S0385-8146(01)00135-3
35. Costello R, O'Callaghan T, Śbahoun G. Éosinophiles et réponse antitumorale. *La Rev Médecine Interne*. 2005;26(6):479–484. doi:10.1016/J.REVMED.2005.02.013
36. Rothenberg ME, Hogan SP. The eosinophil. *Annu Rev Immunol*. 2006;24(1):147–174. doi:10.1146/ANNUREV.IMMUNOL.24.021605.090720
37. Rosenberg HF, Dyer KD, Foster PS. Eosinophils: changing perspectives in health and disease. *Nat Rev Immunol*. 2013;13(1):9–22. doi:10.1038/NRI3341
38. Ondari E, Calvino-Sanles E, First NJ, Gestal MC. Eosinophils and bacteria, the beginning of a story. *Int J mol Sci*. 2021;22(15):8004. doi:10.3390/IJMS22158004
39. Gonzalez MR, Bischofberger M, Pernot L, Van Der Goot FG, Frêche B. Bacterial pore-forming toxins: the (w)hole story? *Cell mol Life Sci*. 2008;65(3):493–507. doi:10.1007/S00018-007-7434-Y
40. Los FCO, Randis TM, Aroian RV, Ratner AJ. Role of pore-forming toxins in bacterial infectious diseases. *Microbiol Mol Biol Rev*. 2013;77(2):173–207. doi:10.1128/MMBR.00052-12
41. Legrand F, Driss V, Delbeke M, et al. Human eosinophils exert TNF-α and granzyme A-mediated tumoricidal activity toward colon carcinoma cells. *J Immunol*. 2010;185(12):7443–7451. doi:10.4049/JIMMUNOL.1000446
42. Mattes J, Hulett M, Xie W, et al. Immunotherapy of cytotoxic T cell-resistant tumors by T helper 2 cells: an eotaxin and STAT6-dependent process. *J Exp Med*. 2003;197(3):387–393. doi:10.1084/JEM.20021683
43. Mullard A. Can innate immune system targets turn up the heat on "cold" tumours? *Nat Rev Drug Discov*. 2018;17(1):3–5. doi:10.1038/NRD.2017.264
44. Hu A, Sun L, Lin H, Liao Y, Yang H, Mao Y. Harnessing innate immune pathways for therapeutic advancement in cancer. *Signal Transduct Target Ther*. 2024;9(1). doi:10.1038/S41392-024-01765-9
45. Griswold KE, Bailey-Kellogg C. Design and engineering of deimmunized biotherapeutics. *Curr Opin Struct Biol*. 2016;39:79–88. doi:10.1016/J.SBI.2016.06.003

46. Shafiee F, Aucoin MG, Jahanian-Najafabadi A. Targeted diphtheria toxin-based therapy: a review article. *Front Microbiol*. 2019;10:10. doi:10.3389/FMICB.2019.02340
47. Céspedes MV, Unzueta U, Álamo P, et al. Cancer-specific uptake of a liganded protein nanocarrier targeting aggressive CXCR4+ colorectal cancer models. *Nanomedicine Nanotechnology, Biol Med*. 2016;12(7):1987–1996. doi:10.1016/j.nano.2016.04.003
48. Falgàs A, Pallarès V, Unzueta U, et al. A CXCR4-targeted nanocarrier achieves highly selective tumor uptake in diffuse large B-cell lymphoma mouse models. *Haematologica*. 2020;105(3):741–753. doi:10.3324/haematol.2018.211490
49. Rioja-Blanco E, Arroyo-Solera I, Álamo P, et al. Self-assembling protein nanocarrier for selective delivery of cytotoxic polypeptides to CXCR4+ head and neck squamous cell carcinoma tumors. *Acta Pharm Sin B*. 2022;12(5):2578–2591. doi:10.1016/j.apsb.2021.09.030
50. Medina-Gutiérrez E, Céspedes MV, Gallardo A, et al. Novel endometrial cancer models using sensitive metastasis tracing for CXCR4-targeted therapy in advanced disease. *Biomedicines*. 2022;10(7):1–18. doi:10.3390/biomedicines10071680
51. A G. Immunotoxins: a review of their use in cancer treatment. *J Stem Cells Regen Med*. 2006;1(1):31–36. doi:10.46582/JSRM.0101005
52. Lambert JM. Antibody-Drug Conjugates (ADCs): magic bullets at last! *Mol Pharm*. 2015;12(6):1701–1702. doi:10.1021/ACS.MOLPHARMACEUT.5B00302